3

Satellite-Based Snow Cover Analysis and the Snow Water Equivalent Retrieval Perspective over China

Yubao Qiu[1*], Huadong Guo[1], Jiancheng Shi[2] and Juha Lemmetyinen[3]
[1]*Center for Earth Observation and Digital Earth, Chinese Academy of Sciences, Beijing*
[2]*Institute for Computational Earth System Science, University of California, Santa Barbara*
[3]*Finnish Meteorological Institute (FMI), Arctic Research Centre, Sodänkylä*
[1]*China*
[2]*USA*
[3]*Finland*

1. Introduction

Global changing is a great challenge that affects the nowadays world, even arises and becomes kinds of the political issues. The changing of the snow is not only a sensitive factor act as a driving force but can be influenced much in the global temperature variation, especially for the seasonal snow cover which is vastly distributed over the northern hemisphere. Snow cover influences the atmosphere and ocean, and therefore the climate system, through both direct and indirect effects (Judah, 1991). In the climate regime, the snow cover alters the surface energy and water circle in a global scale in the climate processing (Fg.1). From the IPCC (2001), the recent and anticipated reductions in snow cover due to future greenhouse warming are an important topic for the global change community. Large seasonal variations in snow cover are of importance on continental to hemispheric scales induces to investigate its natural variability in the climate-system forcing of such trends, versus possible anthropogenic influences (Roger, 2002). So, understanding the spatial pattern in the temporal variability of snow cover increase the current understanding of global climate change and provide a mechanism for exploring future trends (Steve Vavrus, 2007) . As such, snow cover is an appropriate indicator of climate perturbations and may be a suitable surrogate for investigations of climate change (Serreze , 2000; IPCC, 2001; Roger, 2002; Wulder, 2007; IPCC AR4, 2007).

Recent research result over China area revealed that the long time series snow trend is not suit for the whole trend over northern hemisphere and regional northern American (Qin, 2006; Xu, 2007; Wang, 2008;). From Qin's research (2006) of snow cover for the period of 1951

*Corresponding Author

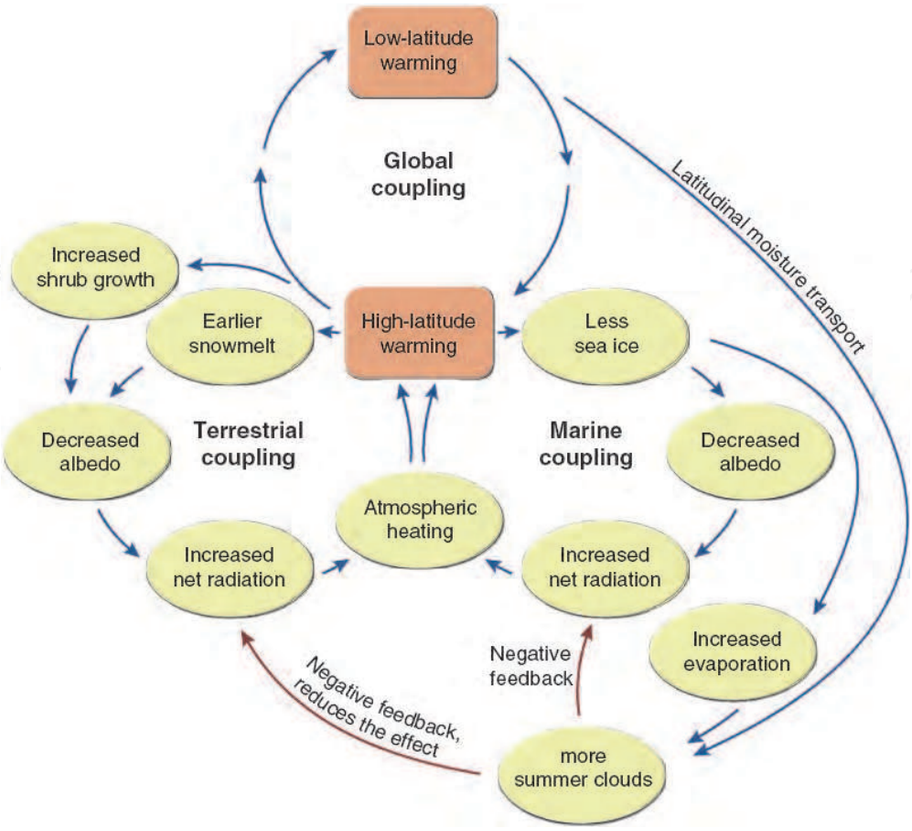

Fig. 1. This conceptual diagram illustrates the connectivity of the positive ice/snow albedo feedback, terrestrial snow and vegetation feedbacks and the negative cloud/radiation feedback. (Source: Chapin III, 2005)

and 1997, the results show that western China did not experience a continual decrease in snow cover during the great warming periods of the 1980s and 1990s. The positive trend of snow cover in western China snow cover is consistent with increasing snowfall, but is in contradiction to regional warming. Xu's result (2007) also show that the SCA of the entire *Tarim* basin in Xinjiang Province revealed a slowly increasing trend from 1958 to 2002, the SCA change in the cold season was positively correlated with the contemporary precipitation change. Wang (2008) reported an inconsistent tend with a reported Northern Hemisphere increasing trend based on limited in situ observations in Xinjiang Province which is a western province in China. While over the area located in the southern parts of the high land of *Tibet Plateau*, China, some investigators explore that annual snow cover has declined by –16% per decade between 1990 and 2001, which is explained due to the contribution of enhanced Indian black carbon (Menon et al., 2010) and the additional absorption of solar radiation by soot on snow cover area (Chand, 2009). Over *Tibetan Plateau* area, Pu's study (2007) indicated that a decreasing trend of snow cover fraction using snow data of 2000–2006 from the Moderate Resolution Imaging Spectroradiometer (MODIS) data is –0.34% per year. In their study, the meteorological station data (Xu, 2007) and the satellite sensor (Scanning Multichannel Microwave Radiometer, SMMR) observed snow depth (SD), NOAA snow cover area data and MODIS snow cover fraction products are used. When concerning the climate change impact on snow cover, the variability of snow cover area is negatively associated with to air

temperature(Wang, 2008), and positive trend of the snow cover area is connected with the increasing precipitation records (Qin, 2006;) in western China. While over *Tibet Plateau* area, China, it is difficult to analyze the long time series trend for its highly rugged mountain, west-east variation and sparse meteorological stations. The data used in these studies are mostly based on the some single satellite products and meteorological station records which are sparse over the high altitude area of *Tibet Plateau*. Furthermore, the meteorological stations are affected by station location, observing practices and land covers, and are not uniformly distributed. Therefore, it is important to evaluate the gross representative satellite data in a large scale area for more than twenty years and try to deliberate the climate impact on the snow behaviors over *Tibet Plateau* area in mid-latitude.

According to the importance of the snow and the climate singularity aspects, in this work, we used the available snow cover area (Snow Cover Area), snow depth (Snow Water Equivalent, SWE) products to examine the climatological characteristics and time series analysis over *Tibetan Plateau* area and study the new snow-retrieval algorithm over China area which often experiences the shallow snow situation. This chapter includes two parts, the first is to analyse the snow products, include the near-time optical and passive microwave remote sensing and the blended SCA and SWE products, the second is to analyse the perspective view of the shallow snow retrieval analysis based on the passive microwave high frequency.

2. Climatology analyses of the satellite-based snow parameters over China

2.1 Introduction

The climatology features for a long time series of snow parameters over land could provide the signature of climate changes across the globe. According to the IPCC AR4 report, the snow extent is sharply decreasing over Northern Hemisphere from the prediction of the nine General Circulation Models since 2000. This part provides a climatology analysis of the SCA and SWE over China area and *Tibetan Plateau* from the satellite observation. The data set includes snow extent and snow water equivalence. Snow extent products are 24 km daily Northern Hemisphere snow and ice coverage from the NOAA/NESDIS Interactive Multi-sensor Snow and Ice Mapping System (IMS), Near-Real-Time SSM/I-SSMIS EASE-Grid Daily Global Ice Concentration (NISE) and Snow Extent and the Moderate-resolution Imaging Spectroradiometer (MODIS, TERRA/AQUA) snow cover fraction (SCF) products from 1999 to now, and the SWE products include Global Monthly EASE-Grid Snow Water Equivalent Climatology from 1978 to 2007, and the Advanced Microwave Scanning Radiometer for EOS (AMSR-E) from 2002 to now. The SCF (MODIS) and SWE (AMSR-E) are employed to analyse the ten years' time series over *Tibetan Plateau* (the area is defined by the area where the atmosphere pressure is less than 700 hPa).

2.2 Satellite–based snow products and processing method

2.2.1 Snow extent and snow cover fraction products

a. IMS Daily Northern Hemisphere Snow and Ice Analysis at 24 km Resolution

This data is 24 km daily Northern Hemisphere snow and ice coverage by the NOAA/NESDIS Interactive Multi-sensor Snow and Ice Mapping System (IMS) (National Ice Center, 2008). The key parameters for this type of data are listed below:

- Time Span: 1997~2011
- Polar Stereographic Projection
- 1024*1024 grid
- Spatial Resolution :~24km
- Time frequencies: Daily
- Four types parameters: Ocean\Land\Sea ice\Snow
- Optical satellite and other sources (environmental satellite imagery)
- Distorted much in China Area

From the sample data map in fig.2, we can find that the SCA data is distorted over China area. Over the northern hemisphere, the China area is not a dominant domain in the continent analysis. It is fit for the onset, duration and end of the snow for its daily resolution.

b. Near-Real-Time SSM/I-SSMIS EASE-Grid Daily Global Ice Concentration and Snow Extent

The Near-Real-Time SSM/I-SSMIS EASE-Grid Daily Global Ice Concentration and Snow Extent product (Near-real-time Ice and Snow Extent, NISE) provides daily, global near-real-time maps of sea ice concentrations and snow extent. They are derived from the passive microwave data from the Special Sensor Microwave Imager/Sounder (SSMIS) on board the Defense Meteorological Satellite Program (DMSP) F17 satellite (Nolin, 1998).

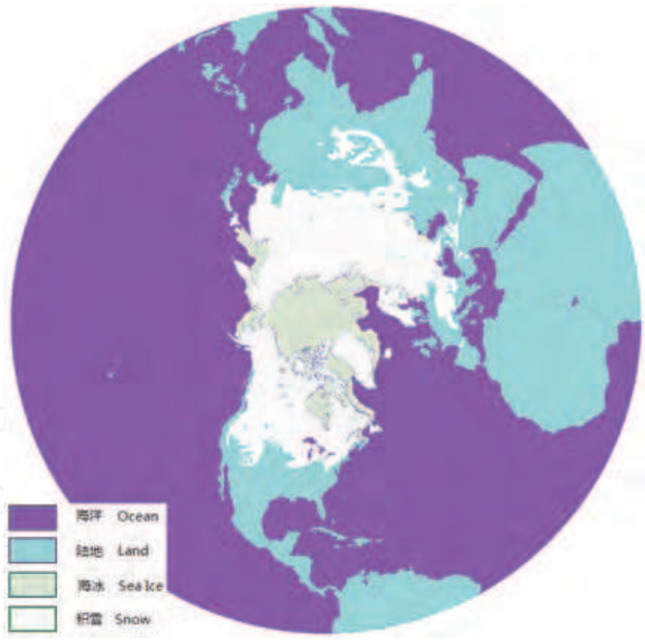

Fig. 2. The sample product from the 24km IMS SCA products, the SCA over China is obvious for its Plateau shape in the upper part of the map

- Time Span: 1995.05~2011.08
- EASE-Grid Projection.
- 721*721 grid
- Spatial Resolution :~25km

- Parameters : Snow extent, Sea ice concentration
- Time frequencies: daily
- NISE Product Source: passive microwave remote sensing data
- Distorted much in China Area

The snow cover over China is showed in the right part of the EASE-GRID projection image (Fig. 3), which is also distorted for some extent. The data could be used to evaluation the onset, duration and end of the snow appearance.

c. MODIS/Aqua Snow Cover 8-Day L3 Global 0.05Deg Climate Modeling Grid (CMG)

The MODIS Snow Cover 8-Day L3 Global 0.05Deg CMG (Fig. 4.) is a global map of snow cover expressed as a percentage of land, i.e. snow cover fraction, in each CMG cell for an eight-day period, which are derived from the Normalized Difference Snow Index (NDSI) of MODIS spectro-radiometer data (Hall, 1995). The percentage of snow-covered land is based on the clear-sky view of land in the CMG cell, and count the number of snow observation over land. So the amount of snow observed in a CMG cell is based on the cloud-free observations mapped into the CMG grid cell for all land in that cell (Hall, 2007). Compared with the daily snow-cover products, the eight-day SCFs products greatly reduce the percent of cloud obscured or masked pixels from near half to less than 7% over *Tibet Plateau* (Riggs, 2003), which is more suitable to analyse the trend for at a long time span.

- Time span: 2002 to 2010
- Latitude/longitude projection
- Grid resolution is 0.05 degrees
- Parameters: Snow cover fraction
- Time frequencies: eight days
- Source: MODIS optical remote sensing under cloud-free condition
- Suit for the CMG projection

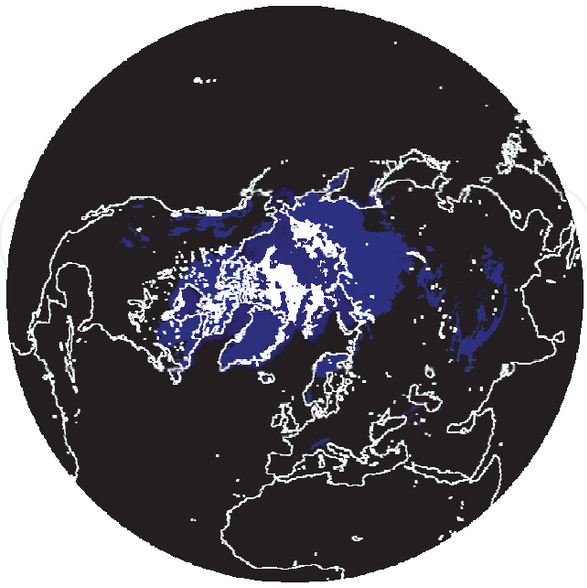

Fig. 3. The sample product from the NISE products, the SCA over China is also obvious for its Plateau shape in the right part of the map (EASE-GRID)

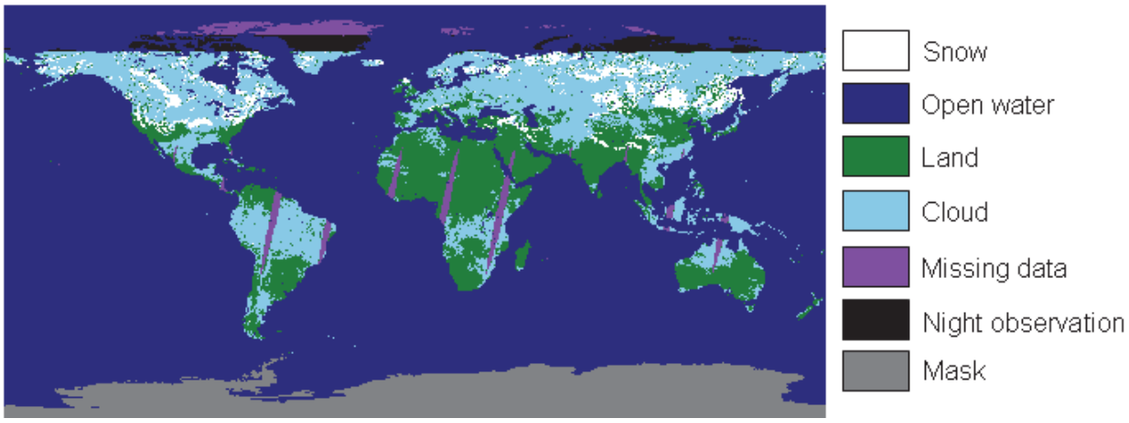

Fig. 4. Sample image derived from MODIS/Aqua Snow Cover Daily L3 Global 0.05Deg CMG data set 08 February 2004 (cited from http://nsidc.org/data/modis/data_summaries/cmg_sample.html)

2.2.2 Snow water equivalent products

a. Global Monthly EASE-Grid Snow Water Equivalent Climatology

This data set comprises global, monthly SWE from November 1978 to 2007, with periodic updates released as resources permit. Global data is gridded to the Northern and Southern 25 km Equal-Area Scalable Earth Grids (EASE-Grids) (Fig.5).

- Time Span: 1978 – 2007
- EASE-Grid Projection.
- 721*721grid
- Spatial Resolution :~25km
- Time frequencies: Monthly
- Parameters : Snow water equivalent and Snow cover frequency of occurrence
- Source: Scanning Multichannel Microwave Radiometer (SMMR) and selected Special Sensor Microwave/Imagers (SSM/I) and Visible snow parameters as a factor
- Distorted much in China Area

b. AMSR-E/Aqua L3 Global Snow Water Equivalent EASE-Grids

We also use the AMSR-E snow products to check the SWE variation and climatology over *Tibet Plateau*. The SWE_Northern daily data (Tedesco, 2004) is used in the next process. The data characteristics are listed.

- Time span: 2002~2010
- EASE-Grid Projection.
- 721*721grid
- Spatial Resolution :~25km
- Time frequencies: Daily
- Parameters: Snow Water Equivalent (mm)
- Source: AMSR-E passive microwave remote sensing
- Distorted much in China Area

This data are processed into the maximum and average SWE for the *Tibet Plateau*.

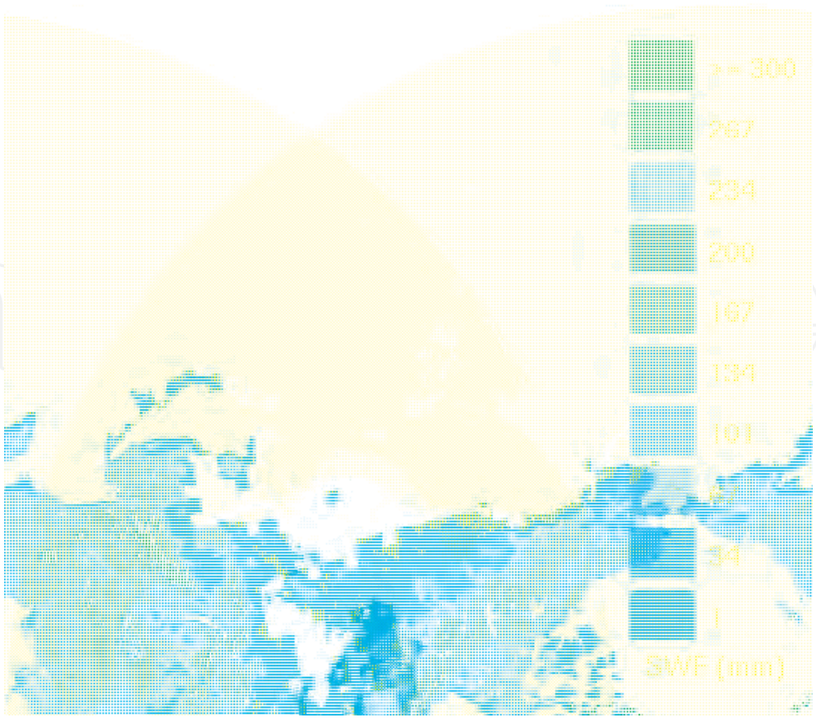

Fig. 5. Northern Hemisphere average snow water equivalent (mm) from passive microwave, with additional area indicated as snow by Northern Hemisphere EASE-Grid weekly snow cover in red, March, 2003.(cited: http://nsidc.org/data/docs/daac/nsidc0271_ease_grid_swe_climatology/NL200303.NSIDC8.BP_VIS35.png)

2.2.3 Multisource satellite data processing method

According to the data characteristics mentioned above, the different projections and resolutions data need to be projected in the same project that could provide a same base for the later analysis. We select the equal latitude and longitude project to provide a more effective understanding for the China mid-latitude area. A tool has been developed to processing the EASE_Grid, Polar Stereographic Projections into the 0.05 degree latitude and longitude map. Fig. 6 shows the transform scheme from the multi-projection to the equal latitude and longitude.

When all of these data products are resampled, we analyse the onset and duration of the data from the SCA products (named: IMS and NISE) using the accumulating, the first and the end day of the snow. The monthly SWE products are used to calculate the climatological characteristics over China by the averaging method.

2.2.4 Onset, duration of the snow cover over China

After all of the data mentioned above is projected into the same equal latitude and longitude grid. The IMS and NISE daily snow cover data are processed to the onset, duration and the end time map, the base-time for IMS product is 31/May, and the day of the year 183 (almost 31/May) for NISE products. The Global Monthly EASE-Grid Snow Water Equivalent

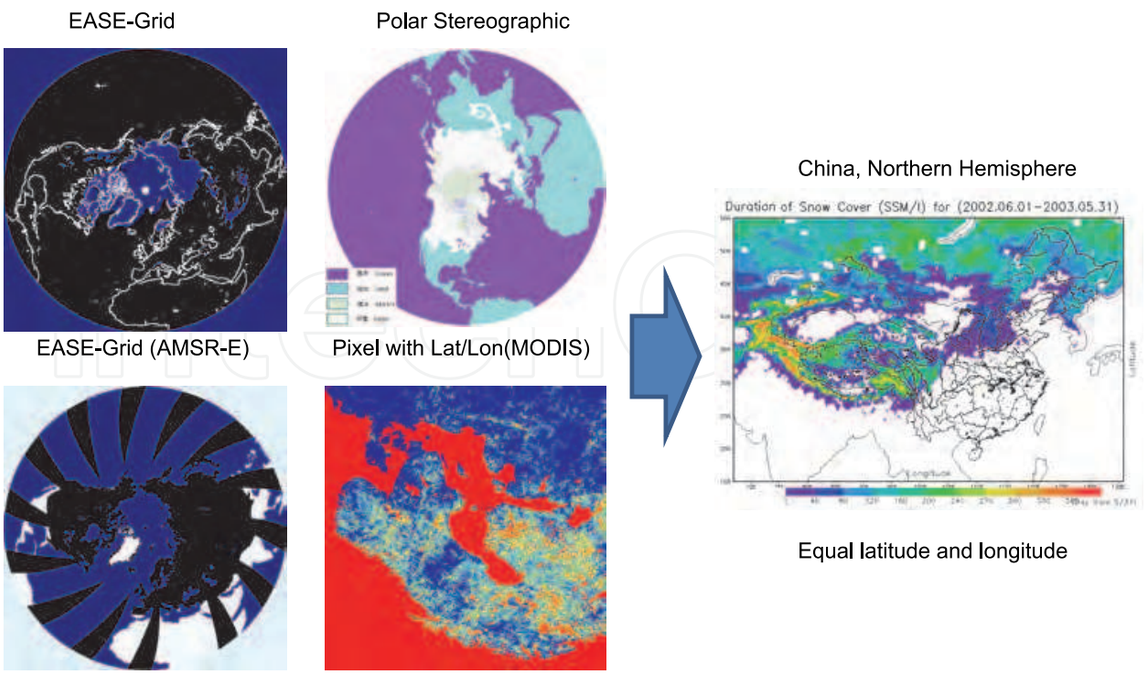

Fig. 6. The resampling processing in the transition process (multi-projection to equal latitude and longitude)

Climatology data is reprocessed to analyse the averaged monthly climatologic characteristics. The data quality control has been done to make sure that the representativeness suit for statistical analysis. The China area is defined as 15^0N-56^0N, and 67^0E-136^0E, includes all of the Chinese land area, part of the center-Asia, Mongolia, and part of the southern Russia, where the snow often appear.

a. Onset of the snow cover over China

The onset of the snow cover is plotted using the data from IMS and NISE products for fourteen (1997~2011) and sixteen (1995~2011) at whole year respectively (Fig.7 just shows the corresponding 4 years of these two dataset). From fig.7, the snow cover over Tibet High Mountain and the Centre Asia Mountain is always influenced much by the mountain glaciers, the mostly early snow are showed in the northern part and *Tibet Plateau* area of high mountains marked the permanent snow area (the onset data value is 1). Along with the latitude which changes from south to north, the snow appearance shows its latitude dependency over land area, the high latitude experience early snow cover compared to the low latitude area. The NISE and IMS onset of the snow cover all show postpone in the first snow occurrence, while the IMS records give an explicit result.

These two products show the same regime of the onset of the snow cover but they have explicit difference when compare together (compare these two column in fig.7). The data from NISE take larger area as blank or snow-free area, such as the Yellow River area at Central Plains China. There is more snow record at the beginning of the 31/May at the south margin of the Tibet Plateau that is not suit for the rain forest area in the Northern Indian Mountains. Over the Khrebet Kropotkina area and the northern glacier rich areas the NISE products show the early records about the snow appearance. Overall, the NISE

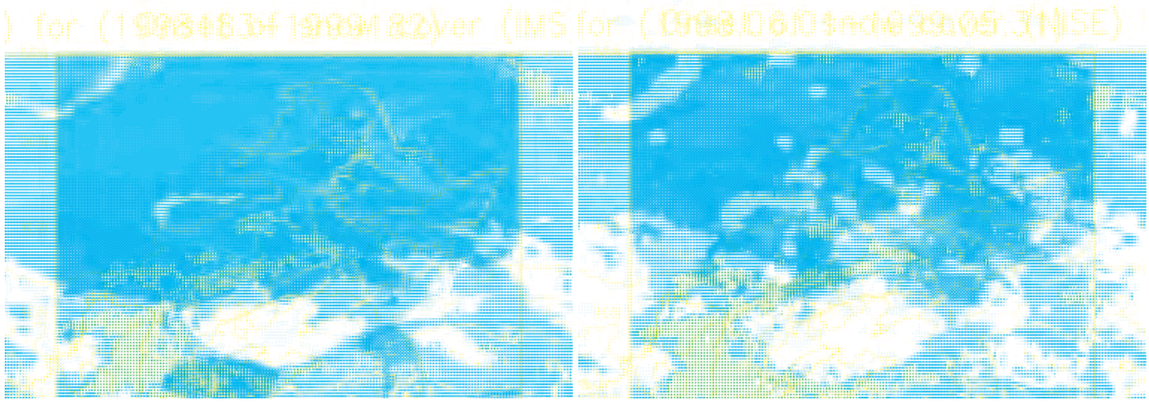

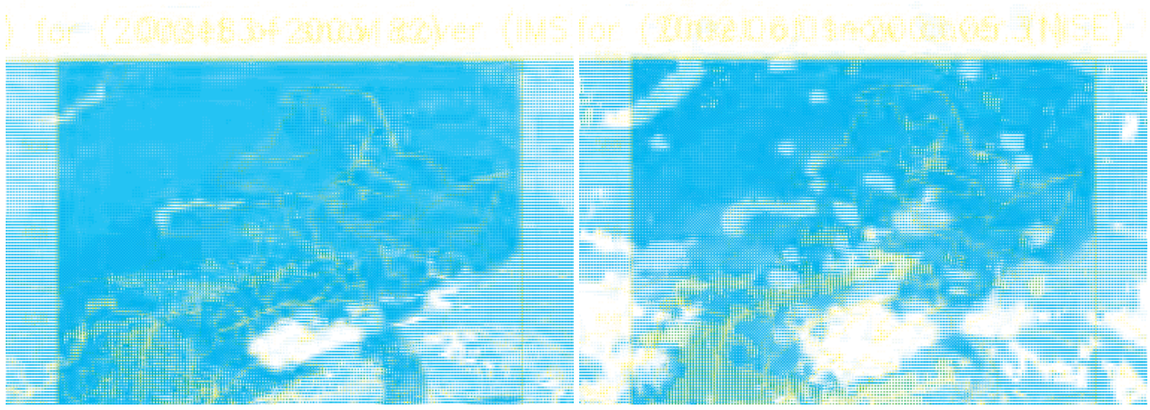

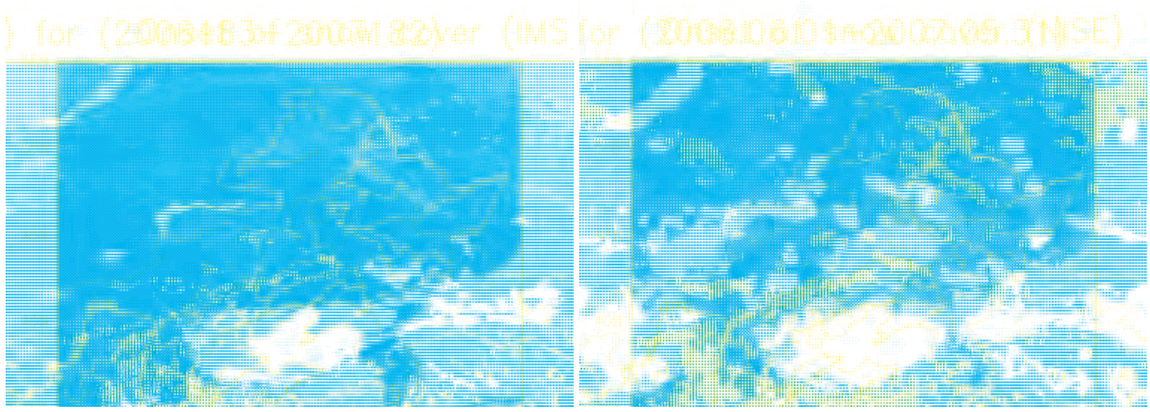

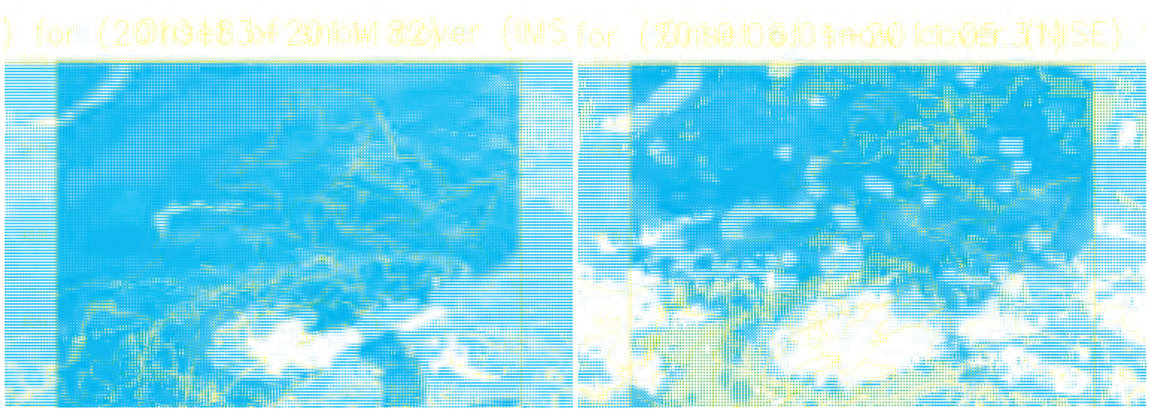

Fig. 7. The onset time of the snow appearance over China, left column is from the IMS products, and the right column is from NISE products. We just give the winter of 4 years, 1998-1999, 2002-2003, 2006-2007 and 2010-2011.

products give out a relative late onset time than that of IMS over flat area which could be attributed to the rugged mountain's influence in the microwave signal in NISE. While for the IMS products, the coverage area are larger than that from NISE (SSM/I) products, and show the early first snow occurrences. The IMS spatial distribution of the snow are possibly more accuracy than that of NISE, such as the Korea Island and the southern China where there is snowy in the January or February.

b. Duration of Snow cover over China

The duration of snow cover for a region is also a sign of climate condition. The duration of the snow is derived from the snow products, IMS and NISE. From fig.8, the duration distribution of the snow is inhomogeneous. The high land area experiences the longest time of the snow cover, such as the expected *Tibet Plateau* and the northern glacier rich area. The duration of the snow have direct relationship with the latitude (higher latitude, longer snow duration), and the southeastern China has the least time of snow cover where the climate is temperate continental climate.

The snow duration data from these two dataset are similar distributed but the NISE (i.e. SSM/I) product shows the longer time when compare the same region in the lower latitude at high land, for example, the snow over Tibet Plateau. Over the high latitude area, the time-span of the snow existence from IMS is somewhat longer than that from NISE. These aspects reveal that the satellite snow products of optical and microwave estimation are different in northern part of China and high land of Tibet Plateau, which is similar with the finding of Wang (2007).

From fig.8, the time series of the snow cover duration is increasing over the patchy snow cover areas, such as the low land of the China area, e.g. south-east of China and the Yellow river area. It seems that there is somewhat a little bit of longer and longer duration of the

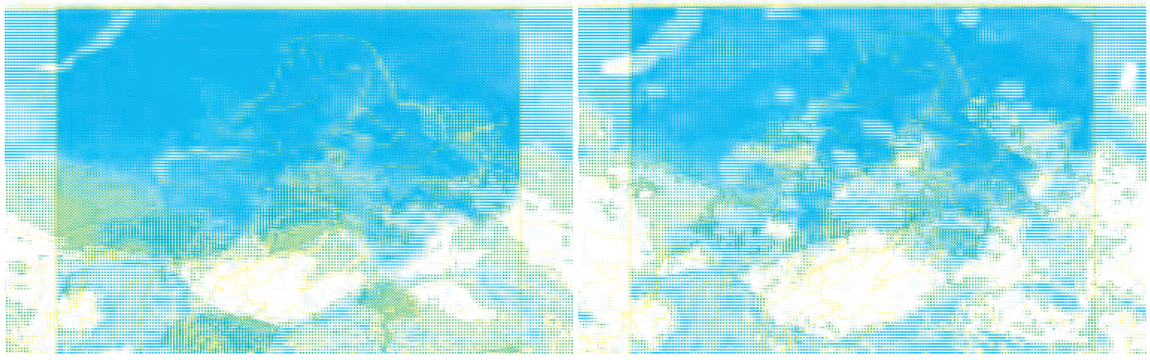

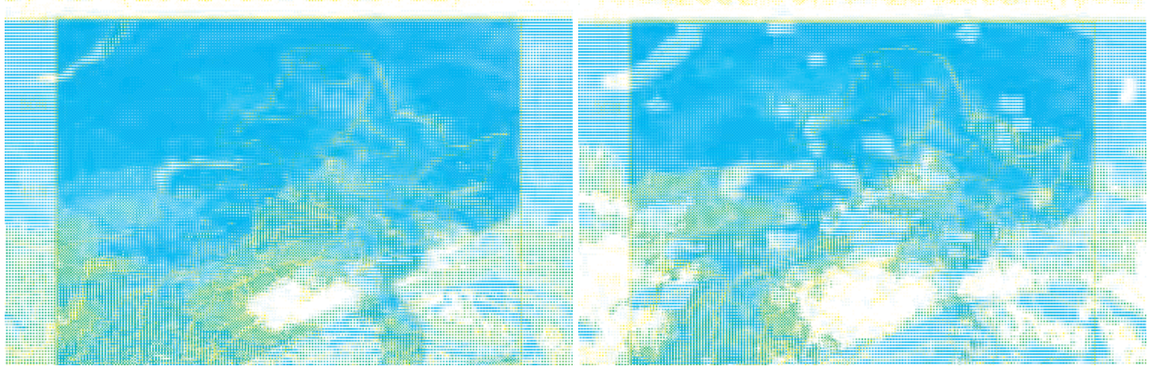

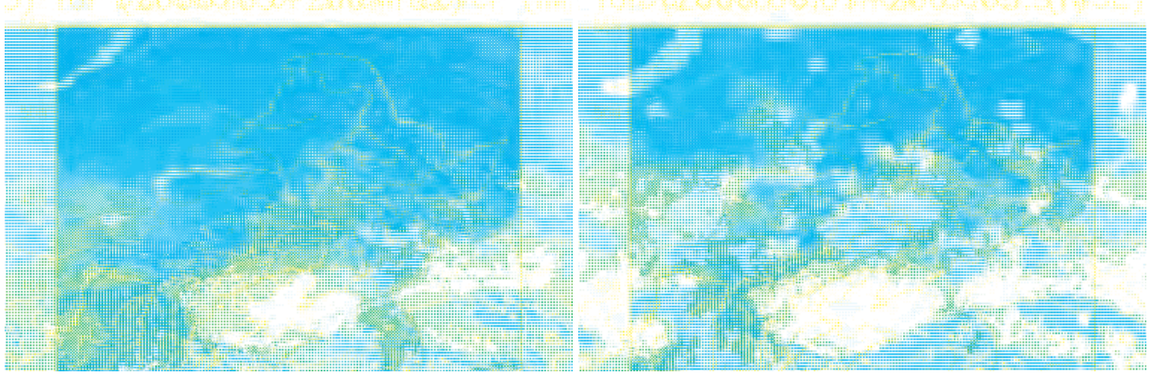

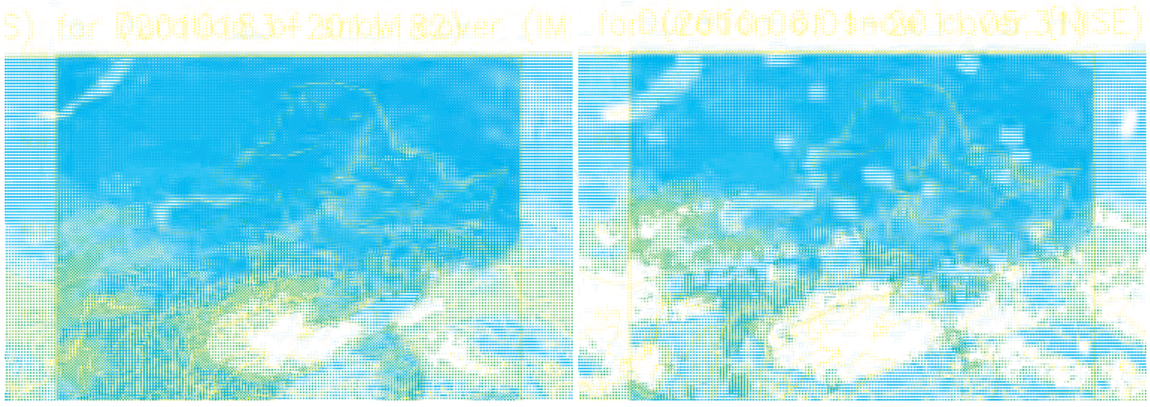

Fig. 8. The duration of the snow appearance over China, left column is from the IMS products, and the right column is from NISE products

snow over Tibet Plateau area from IMS records for fourteen years, but an ambiguous trend is for the 14 or 16 years. Over the southeastern China, the snow obviously exits in every winter time, but the NISE products does not record for its empirical ancillary data in the algorithm, we could get that the data from IMS is more reliable for the situation over China than that from NISE (SSM/I).

c. The monthly climatologic characteristics over China

The monthly snow climatology map is derived from the EASE-Grid Snow Water Equivalent (SWE) for about 30 years' satellite records. From fig.9, the seasonal snow change is obvious in the most area of China. The winter and early spring time from December to the March of next year is the snowiest over the northern China. The maximum snow cover area is in January. From May to September, the snow cover became less and less except the high altitude of *Tibet Plateau* area. The minimum snow cover area is in August. While the maximum SWE and snow cover area of northern China and *Tibet Plateau* area is quite different, the SWE (mm) reach its peak in November over *Tibet Plateau*, and the northeastern China suffered its maximum SWE (mm) in February. The snow cover area in Qinghai-Xizang (Tibet) experiences the largest snow cover in January, which is consistent with Qin's result (2006), while the western area (Xinjiang province) of China reaches its maximum snow in February along with the maximum SWE (mm) which is earlier than that of Qin's (2006). The southeastern China is almost snow-free for the all year time.

The climatological characteristic of *Tibet plateau* area is different than that of the low land area of China, especially the northern part of China. The latitude dependency is obvious in the northern China. Another control factor is the altitude, especially over the Northern Mongolia when compared with the ASTER Global Digital Elevation Map (http://asterweb.jpl.nasa.gov/images/GDEM-10km-colorized.png).

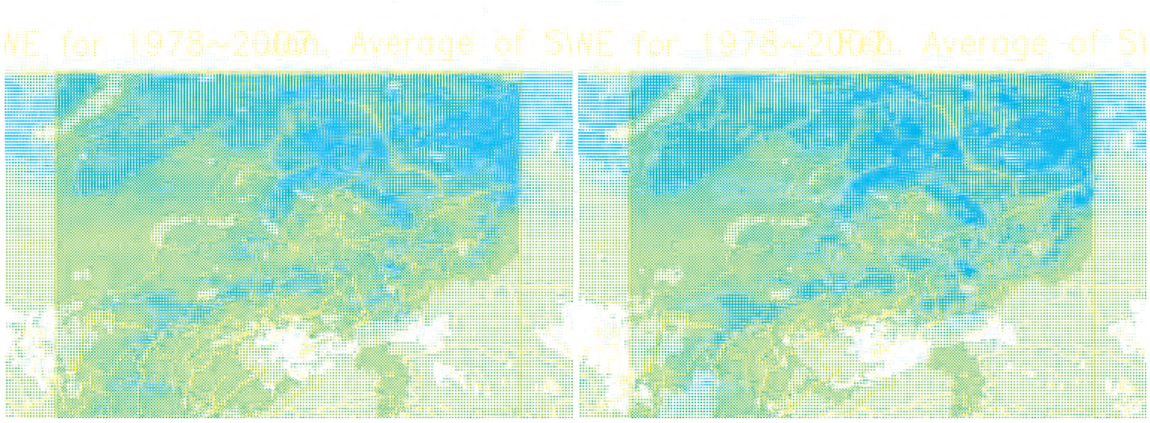

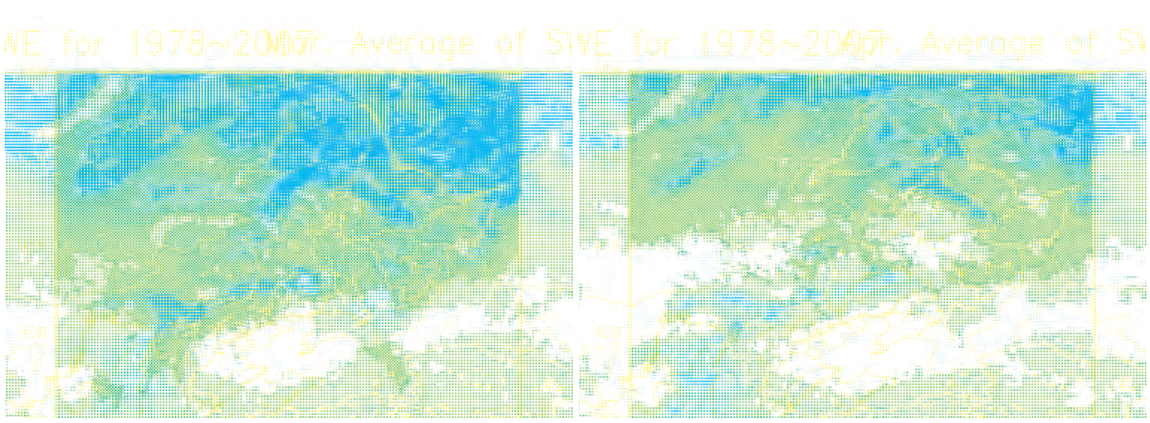

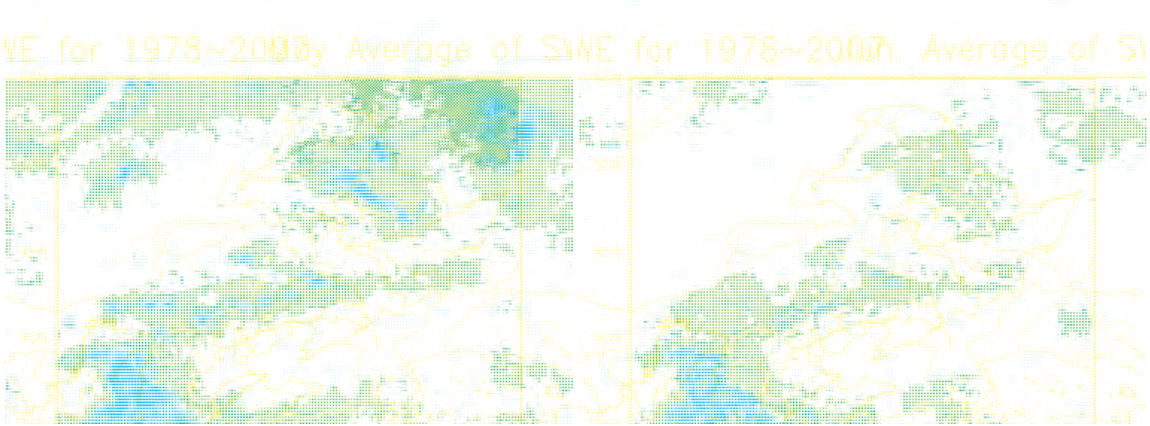

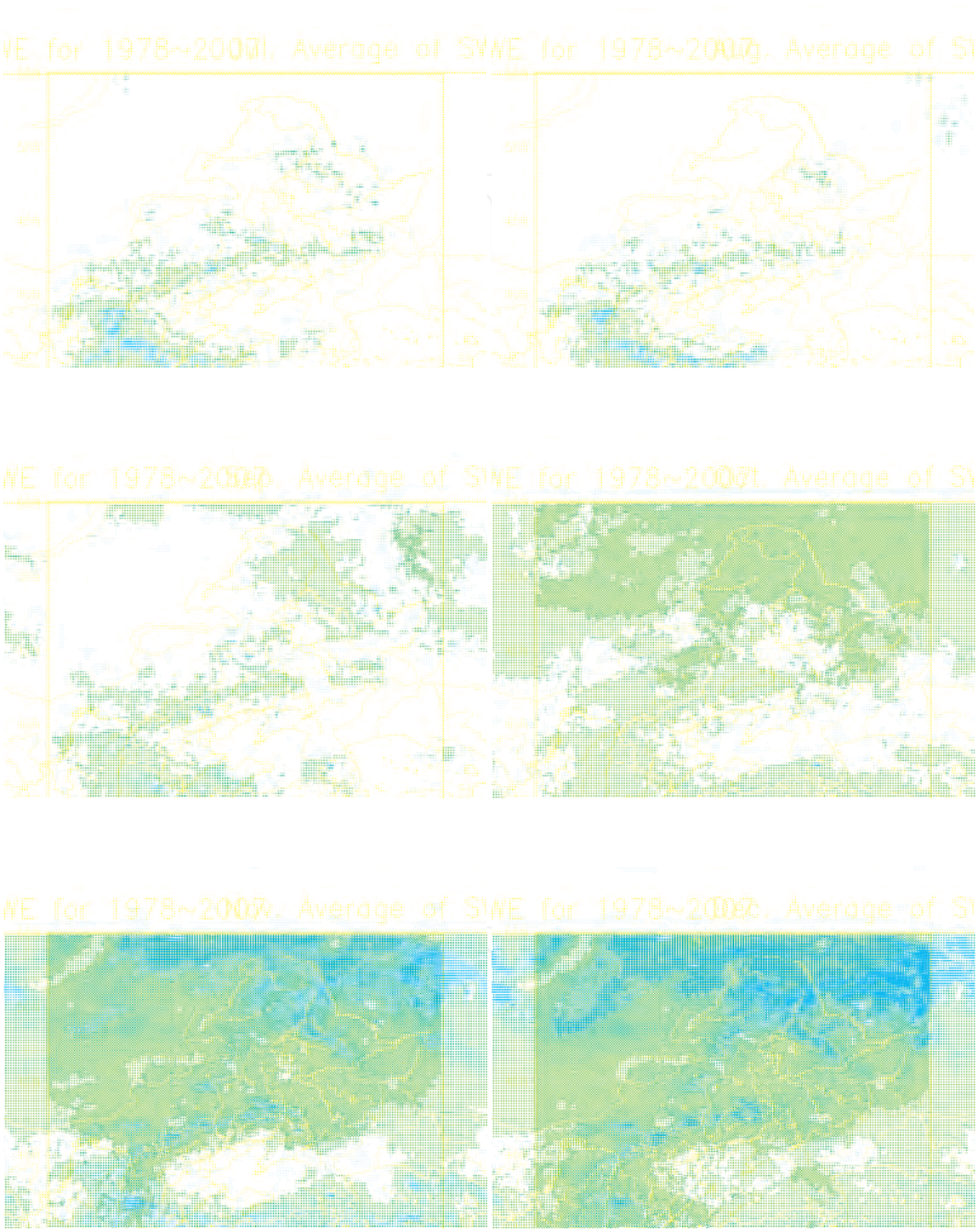

Fig. 9. The monthly averaged SWE (mm) of the snow appearance over China, data is from Global Monthly EASE-Grid Snow Water Equivalent Climatology for 1978-2007

2.2.5 SWE from AMSR-E/Aqua and SCA MODIS/Terra (Aqua) over Tibetan Plateau for the last ten years

From the above analysis, the Tibet Plateau area is quite special in the seasonal snow cover not only for the SCA (Squa. km) but also for the SWE (mm). We consider the high land of *Tibet Plateau* as one whole area by filtering the atmosphere pressure that is lower than 700 hPa, which includes all of the Tibet, China, part of the Qinghai province and the Center Asia mountain areas (see Fig.10). The AMSR-E/Aqua L3 Global Snow Water Equivalent EASE-Grids and the MODIS/Aqua Snow Cover 8-Day L3 Global 0.05Deg Climate Modeling Grid (CMG) data are employed to analyse the snow time series trend over the Tibetan Plateau area.

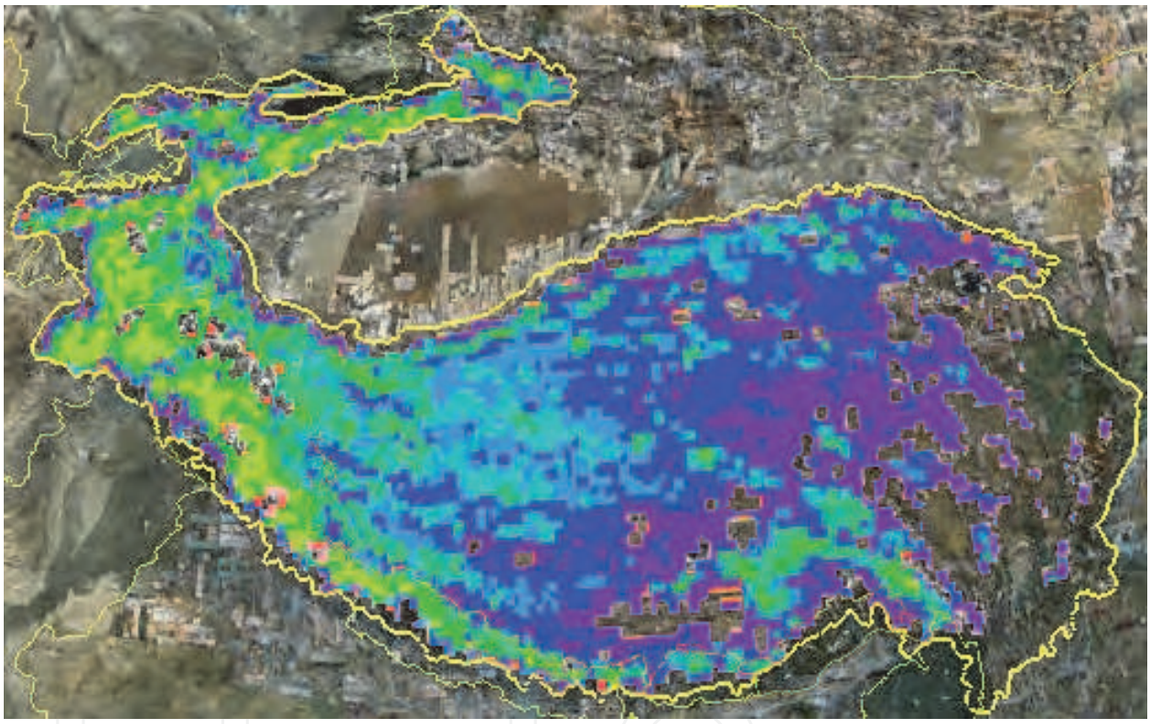

Fig. 10. Definition of *Tibet Plateau* area- according to the air pressure (when < 700hpa)

a. Time-series climatological analysis

The AMSR-E/Aqua provides 8 years' monthly average SWE for the study area, and the total area of the pixels covered by snow is also presented monthly. The time series analysis is in Fig.11, which give a slightly increasing trend for 8 years from 2002 (launch time) to summer, 2010. From fig.11, the average monthly SWE (mm) reach the max value in February (2002/2003, 2003/2004, 2005/2006, 2009/2010) or March (2006/2007, 2007/2008, 2008/2009), and the minimum value appear in August except the summer in 2005, which is quite similar with the section in 2.2.4 c. When we check the SCA from AMSR-E/Aqua, the SCA (Squa. km) reach its maximum extent in January except the winter of 2005/2006, the minimum extent is in July (2002, 2005, 2008) or August (2003, 2004, 2006, 2007, 2009). These tells a positive trend of SCA and SWE over the high altitude region (<700hpa) of *Tibet Plateau* area.

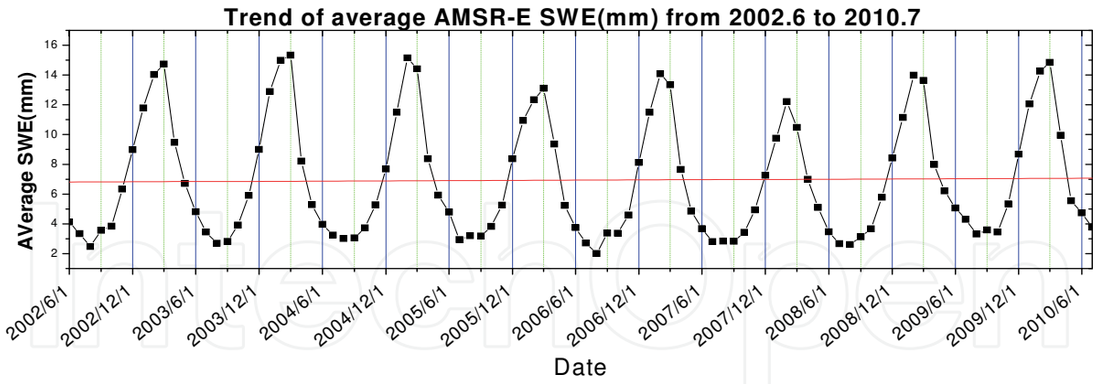

Fig. 11. Time series of the averaged AMSR-E Snow Water Equivalence (SWE) (Average snow cover area, the SCA plot is not showed here).

b. The monthly averaged SWE (mm) and SCA(Squa. km) from 2002.6 to 2010.7

The time series analysis for the averaged SWE (mm) is presented in Fig.12, the fluctuation for each month in the near eight years is small but can find that the slightly trend (see Table 1). The trend analysis shows that the SWE (mm) experience a slightly increasing in this eight years from June to September, which is almost in the summer and autumn time of one year in China, while other time (winter and spring) are decreasing in the averaged SWE (mm). The SCA parameter of the study area shows the same trend as the averaged SWE (see table1 at right column). This climatological characteristic is fit for the Warming and Wetting of the *Tibet Plateau* (Bao, Q., 2010) for the increasing precipitation in the summer time, while the increasing precipitation could not influence the winter and spring snow-rich situation.

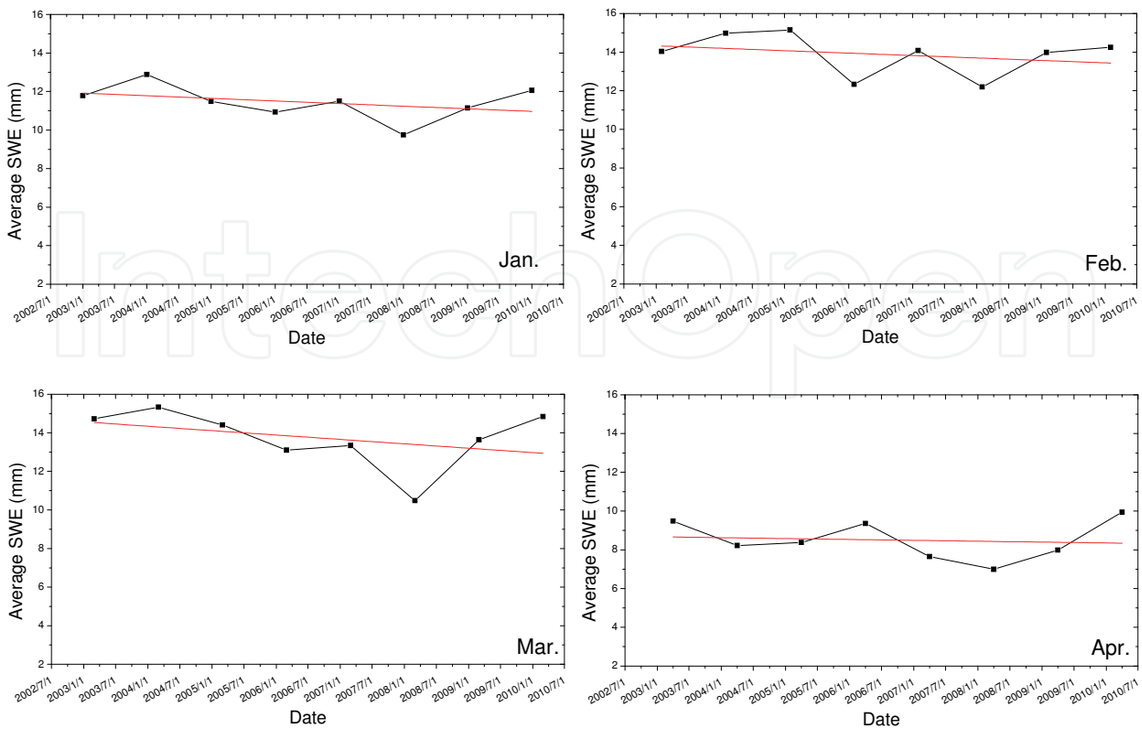

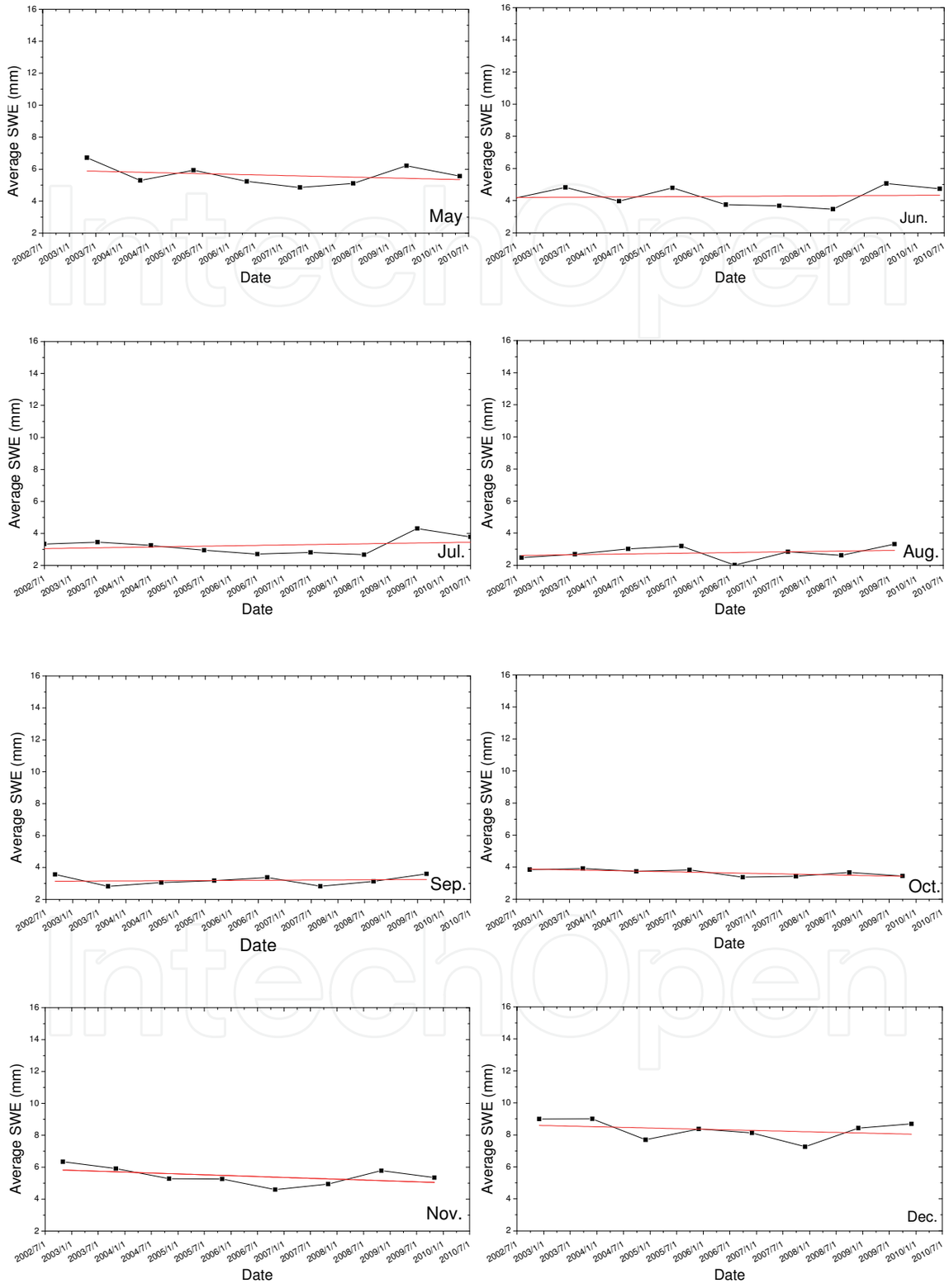

Fig. 12. The time series of average SWE (mm) for twelve months in one year

Month	Rate of Changing Averaging SWE (mm)	Rate of Changing SCA (Squa. KM)
Jan.	-0.00037	-7.36287
Feb.	-0.00035	-17.9450
Mar.	-0.00062	-17.4998
Apr.	-0.00012	-29.1789
May	-0.00021	-89.2610
Jun.	0.000049	26.7051
Jul.	0.00014	23.9970
Aug.	0.00012	20.2665
Sep.	0.00004	-48.7194
Oct.	-0.00017	-14.1196
Nov.	-0.00030	21.7514
Dec.	-0.00021	-2.1661

Table 1. The trend slope for the average SWE (mm) and SCA (Squa. km) from AMSR-E/Aqua eight years records

c. The time series of the monthly snow cover fraction

For the snow cover fraction area (SFC) statistic for *Tibet Plateau* study area in Fig.13. The snow data from MODIS/Aqua (Terra) can provide the snow cover fractional distribution in different time at the same day (morning and afternoon). In Fig. 13, the time series of the SCFs are plotted for different span (0-10%, 10-20%, 20-30%, 30-40%, 40-50%, 50-60%, 60-70%, 70-80%, 80-90%, 90-100% and 100%) for two satellites (MODIS/Terra and Aqua). Compared these two figures, the SCF area from Aqua satellite is general larger than that of Aqua with the same seasonal characteristic possibly for its different overpass time (morning and afternoon) at mid-latitude area. The summer time (almost in later August or early September) has the least area for the SCF which is greater than 20%, while the winter time (especially in the February) has the maximum area. When focus on the SCF less than 20%, the situation is a different result than that more than 10%, the summer time has the greater area than that in winter time for these two satellites, due to the summer patchy snow fractional pixels influence the satellite estimation. The time series analysis trends for these different SCF's range are showed in Table.2. The changing rate indicates a positive trend for the last ten year, especially for the large SFC which almost distribute in the high altitude mountain area. The largest increasing rate is the SFC between 90% and 100% which indicate the high mountain area suffering an increasing snow cover because the full cover areas are mostly in the high elevation mountain area. Another aspect is that the changing rate for MODIS/Terra record is larger than MODIS/Aqua's, but the reason has not discovered in this study.

	0-10%	10-20%	10-20%	30-40%	40-50%	50-60%	60-70%	70-80%	80-90%	90-100%	100%
MODIS/Aqua	-0.05629	1.82353	1.62721	1.77621	1.51221	1.54443	2.00536	2.14856	3.00974	7.61426	2.35225
MODIS/Terra	1.52948	1.63037	1.14803	1.2696	1.29663	1.36101	1.52654	1.59566	2.20187	8.62898	4.85512

Table 2. The slope coefficients for different SCF range during ten year (Terra) and eight year (Aqua) running

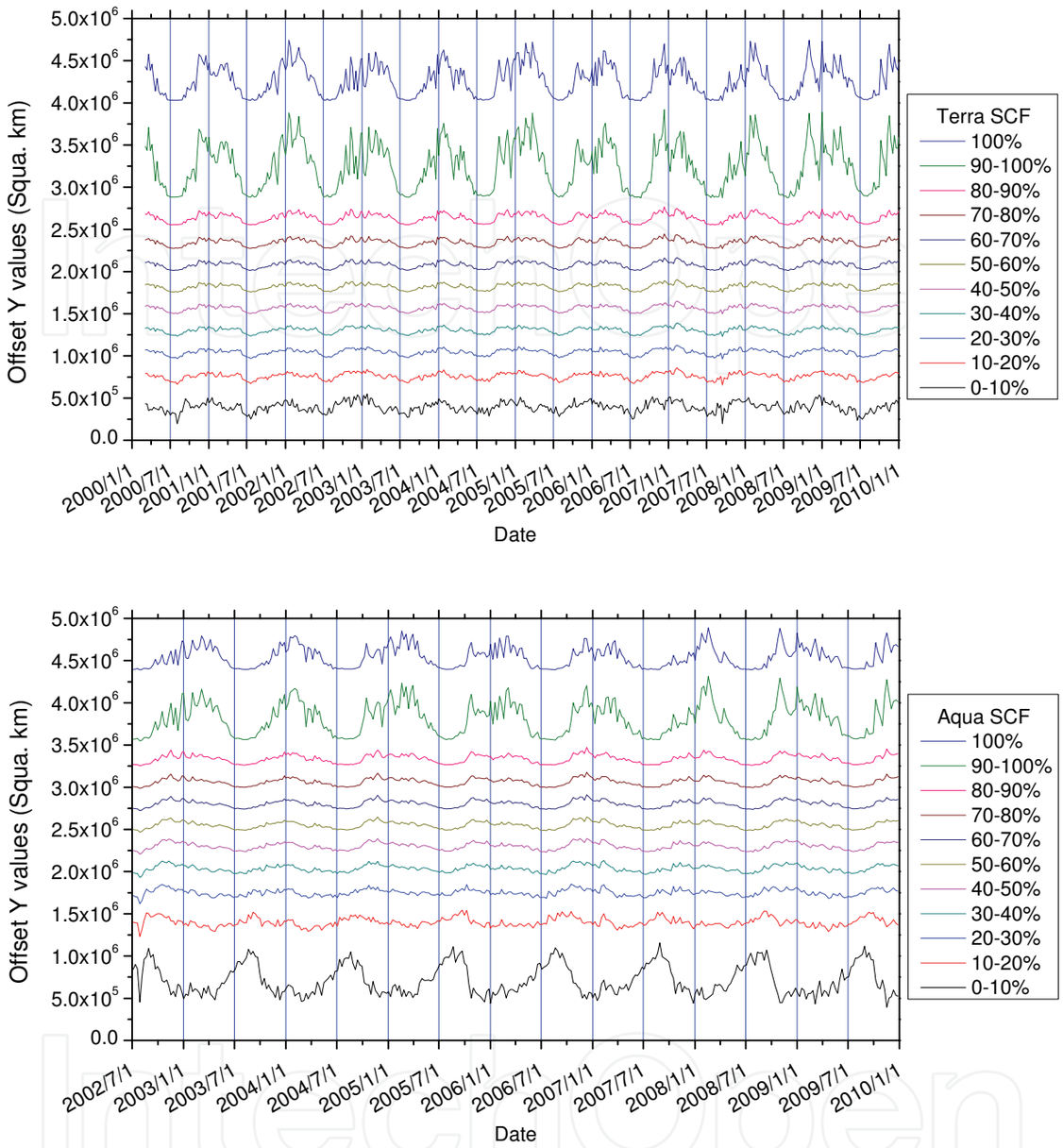

Fig. 13. The time series analysis for different snow cover fractions derived from MODIS/terra and MODIS/Aqua

2.3 Conclusions

From what we have analyzed, the climatological characteristics show that the onset time of snow over China area are slightly postponed, while the duration is undecided by the satellite record of NISE (SSM/I) and IMS, the monthly climatology analysis reveals that the snow distribution is quite different in the altitude and latitude, the Tibet Plateau area experiences the maximum SWE in November. The northern China and lower land reach the maximum area in December and January.

The products of SCA and SWE could provide a long time series data and derived snow climatological analysis, when compared the optical and microwave remote sensing products of snow, IMS SCA and NISE SCA show difference each other, the blank area in Tibet and northwestern China could not enough to provide analytical result, though these are some clues on it. The snow product of IMS seems provide more reliable results over China area, and it is recommended that a new snow algorithm from satellite is needed for the accuracy assessment.

In the traditional view, the satellite data could provide more reliable large-scale snow parameters than the local observational station, the trend from several snow products provides the same continental regime over Northern American, it looks like snow cover gets a negative response to the global warming, while, a near local look over the Tibet Plateau, the result shows that the snow cover area appears a positive trend with snow equivalent water from PSW dataset, and the situation is also same over the China West Area.

From the monthly snow water equivalent (mm) which is recorded from the AMSR-E/Aqua, two snow parameters are derived, one is the averaged SWE monthly and another is the snow cover area (squa. km). The result reveals the positive trend of the averaged SWE (mm) and snow cover area (squa. km) over the Tibet Plateau area, which is the same situation with the result of western China (Qin, 2006 and Xu, 2007). While the monthly trend for more than ten years, we can find some interest results (see b part in 2.2.5). The averaged SWE and Snow cover area experience slightly increasing trend in the summer and autumn time (June, July, August and September), while in the winter and spring time (from October to next May), these parameters shows its negative trend.

From the MODIS SCF time series analysis according to the different percentage pixels, we can find that the SCF less than 20% are quite variable with more pixels in summer time than that in the winter time, while all of the pixels that contain more snow indicate a similar positive trend, and less pixels in summer time than that in winter time. The higher of the SCF, the higher trend value for the line. The data from the MODIS/Aqua show very similar result as that of MODIS/Terra, but larger area than Terra's.

It is hoped that China mainland area whose cryosphere is a major element in the climate now undertake national programs designed to address questions of global environment change.

3. Analysis between AMSR-E brightness temperature and ground snow depth over Tibet Plateau, China

3.1 Introduction

Over the Tibet Plateau (Western China), snow cover is presented only for a few months per year, except mountainous areas. However, it highly influences the energy flux, atmosphere dynamics and surface water reservoirs. Recently, much effort has been put into developing region-specific retrieval algorithms for snow parameter retrieval from passive microwave measurements. Automatic station observations of snow cover are essential factors in the development of these retrieval algorithms, but they cannot provide comprehensive information on the snow cover distribution. The recent study has improved the snow depth accuracy for some extent, but the method highly depend on the method training for the

artificial neural network methodology (Yungang Cao, 2008) without more physical explanation. From the Fig.14, the distribution of the meteorological stations in the Tibet Plateau can be seen to be very sparse, especially over the main part of the Plateau. Furthermore, many of them are near areas of human activity, and provide few measurements for a long time span with very shallow snow depth values (see Fig.15 example for DanXung Station) (Che, 2004). Armstrong (2001) notes that passive microwave remote sensing tends to underestimate the snow in the fall and early winter due to the weak signal of thin snow with the 36.5GHz and 18.7GHz (Armstrong, 2001), while the situation is the opposite over Tibet Plateau. Matthew H. Savoie (2009) improved the accuracy of the snow measurement by considering the atmospheric influence to some extent; Qiu etc. (2009) paid attention to the atmosphere influence via the experiment and model simulation.

Due to the thin snow (snow occurrence) is often seen over western China, especially over the Tibet Plateau, more comprehensive analysis is urgent with the station observation data and microwave Tbs. In this work, we consider the shallow snow situation, and try to explain the discrepancy between the in situ time series measurement of snow (snow depth, SD) and the values retrieved from passive microwave remote sensing with the traditional difference between the brightness temperature at 36.5GHz and 18.7GHz, and that from 89.0GHz-18.7GHz and 18.7GHz-10.7GHz. Then, we analyze the ability of the higher frequencies in snow parameter retrieval over the Tibet Plateau (e.g. 89.0GHz at AMSR-E) using the time series data comparison.

3.2 Snow depth and AMSR-E brightness temperature

3.2.1 Snow depth data

We selected the snow depth measurements at the NamCo station over 4700m in altitude, which is located beside the NamCo Lake and the Mt. Nyainqenttanglha (Fig.14, circle). The Institute of Tibetan Plateau Research, Chinese Academy of Sciences, operates a station in the

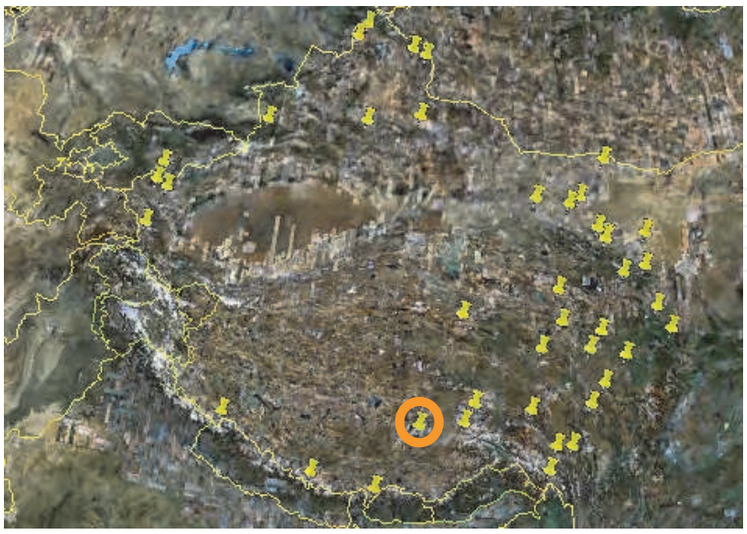

Fig. 14. The distribution of the selected meteorological station over Tibet Plateau and western China (from China Meteorological Data Sharing Server System, data used in this work) and the geographic location of the Namco station site ($30^0$46.44'N, $90^0$59.31'E).

area. A snow campaign covering the whole winter offseason between 2006.10~2007.2 was conducted. SD records are acquired over three sites around the Namco station. Compared to the AMSR-E/Aqua satellite footprint, these sites are regarded as one site and represent the general situation of the whole area in this work, though this is a fairly inaccurate estimation in mountainous areas. Other time-series SD data in this work is from the winter-time observation (stations at Fig.14) in 2009~2010, when northern China were suffered from vast snowfall.

Fig 15 (left) shows a time series of the measured in situ snow depth values. From 24/10/2006, snow depth increases from 23cm to about 45cm on 8/11/2006, after which the depth decreased to 17cm on 28/1/2007. In this time span, several snowfall events happened on 12/11/2006, 14/11/2006 and 16/1/2007, with 2 cm of new snow in the last case. A relatively large shift appeared on 14/12/2006 because of the change of the observation sites for the surface wind.

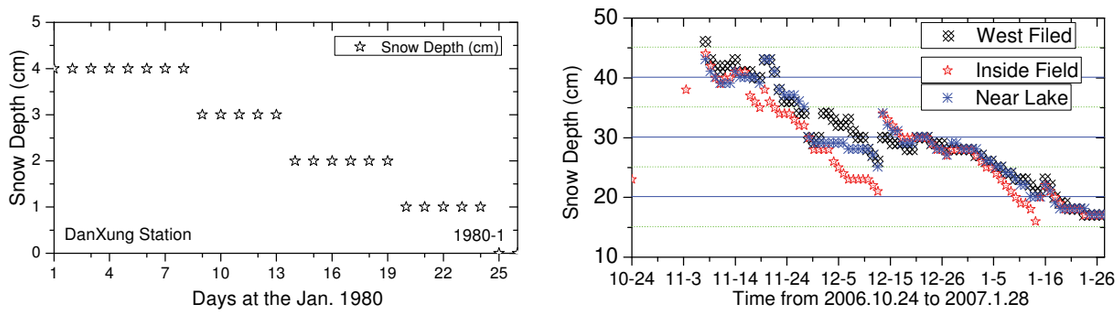

Fig. 15. The SDs from the Danxung station (No.55493) (Left) and the SD (cm) field campaign near NamCo station (Right)

3.2.2 AMSR-E L2A swath dataset and processing

We selected the AMSR-E daily L2A swath brightness temperature (ascending and descending pass, A/D, http://nsidc.org/data/docs/daac/ae_l2a_tbs.gd.html) over the experiment site and other western stations in China according to the geographic coordinate, which means that the extracted swath Tbs are in the area of 10km² around the site. We chose the Tb difference between 89.0/36.5/18.7GHz and 10.7GHz channels for the gradient time series comparison with station snow depth (cm).

3.3 Comparison result at Nam Co experiment site

3.3.1 The AMSR-E swath L2A Tb gradient time series

We plotted the Tb gradient between 89.0/36.5GHz and 18.7GHz with different resolutions corresponding to the snow measurement time at Nam Co in Fig. 15. Compared to the snow depth (the solid lines), the brightness temperature gradient (traditional algorithm prototype) at Fig. 15 shows a good relationship for the snow depth decreasing period (24/11/2006~26/1/2007) at 89.0GHz (named high frequency) gradient and 36.5GHz (named low frequency) gradient. For this period of time (snow depth are less than 30 cm), we can understand that the high frequency are more sensitive to the snow evolution than the low

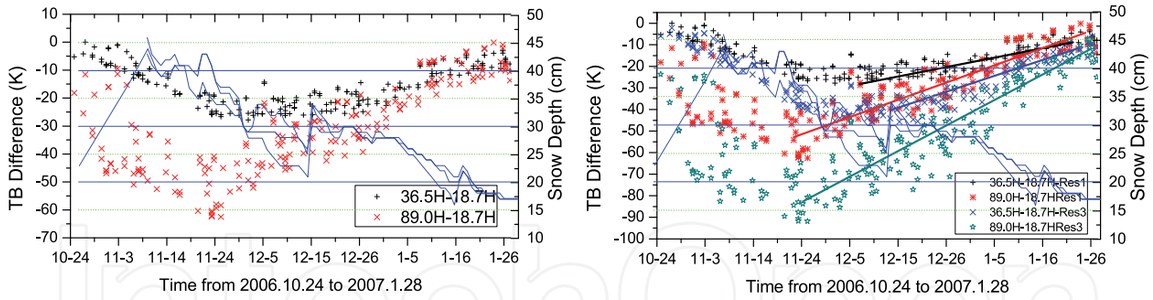

Fig. 16. The brightness temperature gradient between 89.0/36.5GHz and 18.7GHz with different resolution corresponding to the snow measurement time. The solid lines stand for the ground snow depth.

frequency, and the bottom panel in Fig.16 indicates the high resolution (L2A.res3) resample is more sensitive to the snow evolution than that of low resolution (L2A.res1).

Fig.17 shows a sample, located beside (20km away from the field measurement site, the time stamp starts from October 1st), it indicates the same trend as the previous Fig.15. During the first 15days, the 89.0GHz shows a good sensitivity to the fresh snow. During the later succeeding 17days (7/11/2006~24/11/2006), the gradient becomes more and more large, but the snow depth decreases (compare to the Fig.15). This can be explained preliminarily by the evolution of the snow grain size and density, which typically increases with time. A more physical explanation needs e.g. the model simulation work on the snow emission of snow grain size, snow depth and snow density, in order to decide which part plays a dominant role (Pulliainen, 1999).

3.3.2 Comparison to the AMSR-E daily SWE product

Another comparison (Fig.17) has been done by using the AMSR-E daily snow products, which are EASE-Grid with coarse resolution (25km) and the snow depths at Fig.15. From these figures, we can find that the maximum estimated AMSR-E SWE(mm) (using 36.5GHz gradient) over NamCo station at the winter of 2006~2007 occurs around 26/12/2006, which are do not match the snow measurement, with a delay of almost one month.

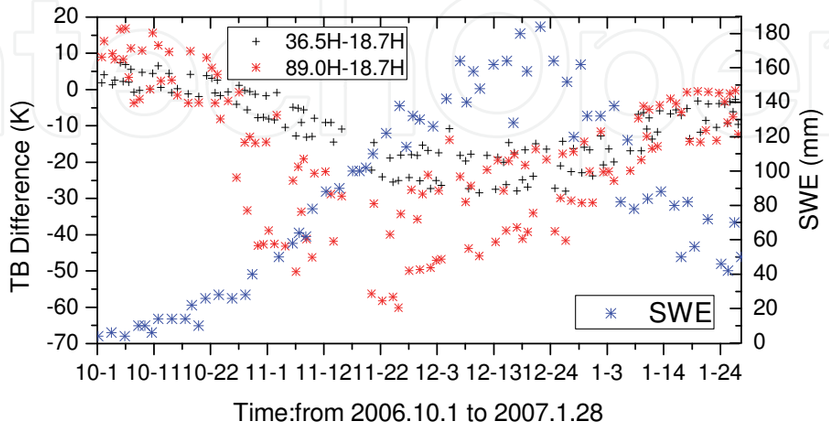

Fig. 17. The AMSR-E SWE daily products (EASE-GRID) and the corresponding TB difference.

Compared with the gradient figure, from Fig.16, we can find that the 36.5GHz gradient shows a relatively stable value from 1/12/2006~26/12/2006. The discrepancy between the SWE and TB gradients is probably due to the response of 37 GHz saturating for SWE values over 120-140mm, or the mixed pixel by the lake. This requires a more extensive field dataset to acquire the explanation.

If we consider the typical snow density over Tibet area to be approximately 0.239g/cm^3, we get a maximum snow depth value of about 75 cm from the AMSR-E observation. This is quite larger compared to the in situ measurements, an indication that the AMSR-E SWE value is overestimated, which is consistent with the result in paper(Pulliainen, 1999).

3.4 Time series analysis between Tb and snow depth

We selected several observations over western China (Fig.14) for the qualitative analysis, which include the Xinjiang and Neimenggu deep snow and Gansu, Qinghai and Tibet shallow snow depth situations.

All of the figures in Fig.18 are plotted with the three gradients (Tb difference at 89.0-18.7, 36.5-18.7 and 18.7-10.7) and the corresponding snow depths (see Fig.18).

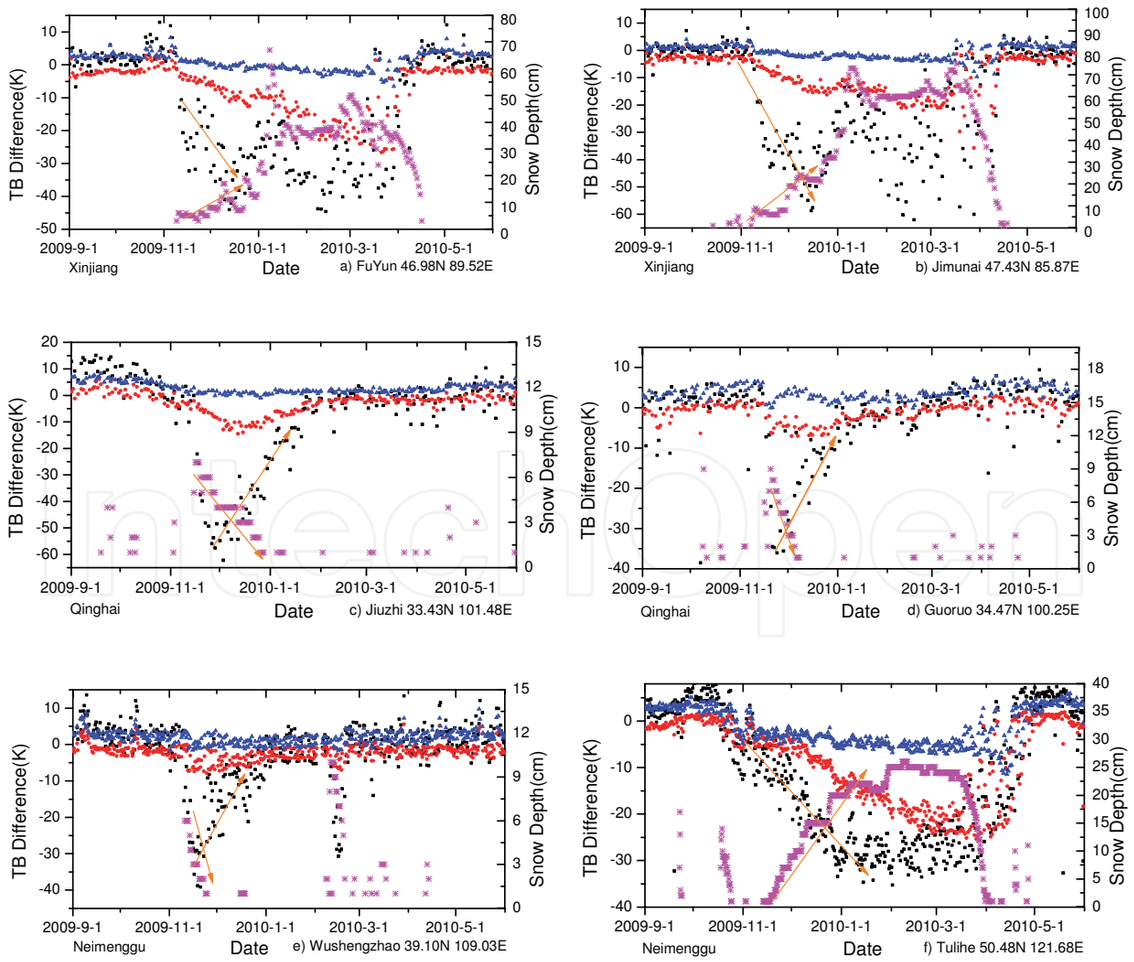

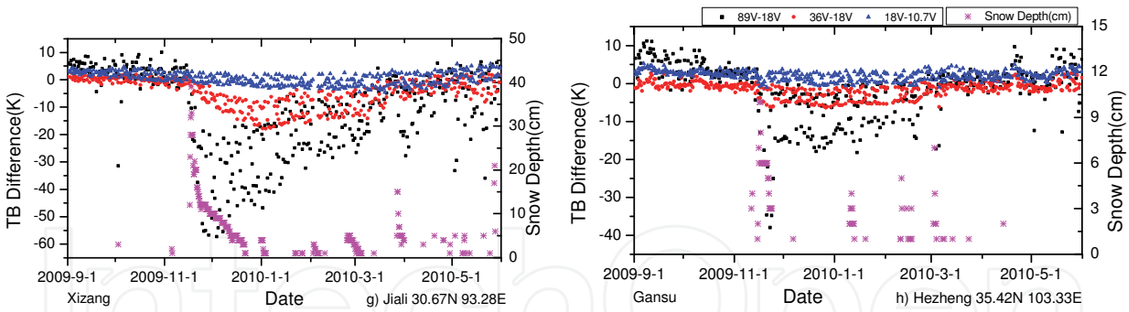

Fig. 18. The time series Tb difference (89/36.5-18.7GHz and 18.7-10.7GHz) and the ground snow depth (cm). The first 4 figures are plotted only ascending Tb and the corresponding ground measurements (local morning time), the last four figures are plotted with all of the Tb (A/D) and snow depth at any available time.

We get the preliminary analysis result, the Tbs at18.7-10.7GHz are insensible to the snow evaluation except the deep snow depth (a, b and f), although the depression in f is obvious due to the local vegetation influence. Over deep snow (a, b, f and g, continuous accumulation > 20cm), the Tbs at 36.5-18.7GHz are more reliable than that of high frequency, while over the shallow snow (c, d, e and h, discontinuous snow occurrence, < 15cm), the pair 36.5/18.7 is insensitive, but the high frequency pair (89.0/18.7) shows its distinct response. The pair 89.0/18.7 shows its shallow snow retrieval ability in a, b, c, d, e and when the snow depth over 20cm, the signal is more variable and suspect. The pair 89.0/18.7 indicates its sensitive response to the quick presence of the snowfall, and keeps turbulence when the snow depths are unchanged due to the temporal snow physical characteristics and climate factors. The last four figures show that the A/D Tbs act the similar behaviors with difference correlation intensity.

3.5 Conclusions

From what we have shown above, it can be argued that the high frequency (89.0GHz) shows its sensitive to the relative shallow snow pack, which suggests that we can develop the shallow snow depth retrieval via the good Tb pair and ground snow depths over the western China. Model simulation work is needed to explain the discrepancy of the snow evolution and brightness temperature gradient at high frequencies, and we should enhance the following aspects, the possible mixed pixel effect, the atmosphere effect elimination, and the vegetation effect removal.

4. Acknowledgement

This work is now supported by the Chinese "973" Program “Earth Observation for Sensitive Factors of Global Change: Mechanism and Methodologies” (NO. 2009CB723906), the Director Foundation of Center for Earth Observation and Digital Earth Chinese Academy of Sciences, the National Natural Science Funds (Grant: 40901175), and the “Open Foundation” of Institute of Plateau Meteorology.

5. References

[1] Armstrong, R. L., & Brodzik, M. J. (2001). Recent Northern Hemisphere snow extent: A comparison of data derived from visible and microwave sensors. Geophysical Research Letters, 28(19), 3673−3676.

[2] Armstrong, R. L., M. J. Brodzik, K. Knowles, and M. Savoie. 2007. Global Monthly EASE-Grid Snow Water Equivalent Climatology. Boulder, Colorado USA: National Snow and Ice Data Center. Digital media.

[3] Basist, A., Garrett, D., Ferraro, R., Grody, N. C., &Mitchell, K. (1996). A comparison between snow cover products derived from visible and microwave satellite observations.Journal of Applied Meteorology, 35(2), 163−177.

[4] Bao, Q., Y. M. Liu, J. C. Shi, and G. X. Wu. 2010. Comparisons of soil moisture datasets over the Tibetan Plateau and application to the simulation of Asian summer monsoon onset. Advances in Atmospheric Sciences 27:303–314.

[5] Cao Yungang, Xiuchun Yang and Xiaohua Zhu, Retrieval snow depth by artificial neural network methodology from integrated AMSR-E and in-situ data—A case study in Qinghai-Tibet Plateau, Chinese Geographical Science, Volume 18, Number 4, 356-360, 2008, DOI: 10.1007/s11769-008-0356-2

[6] Chand, D., Wood, R., Satheesh, S. K., Charlson, R. J., Anderson, T. L.," Satellite-derived direct radiative effect of aerosols dependent on cloud cover", Nat. Geosci., 2,181–184(2009) [doi:10.1038/ngeo437(2009)]

[7] Chapin III, F.S., Sturm, M., Serreze, M.C., McFadden, J.P., Key, J.R., Lloyd, A.H., McGuire, A.D., Rupp, T.S., Lynch, A.H., Schimel, J.P., Beringer, J., Chapman, W.L., Epstein, H.E., Euskirchen, E.S., Hinzman, L.D., Jia, G., Ping, C.L., Tape, K.D., Thompson, C.D.C., Walker, D.A. and Welker, J.M. (2005). Role of land surface changes in Arctic summer warming. Science, 310, 657-660

[8] Che Tao, Li Xin, Geo Feng, Estimation of the snow water equivalent in the Tibet Plateau using passive microwave remote sensing data (SSM/I). Journal of glaciology and Geocryology, vol. 26, no 3, pp.363-368. 2004 (in Chinese)

[9] Cohen, J. and D. Entekhabi. "The influence of snow cover on Northern Hemisphere climate variability," Atmosphere-Ocean, Vol. 39, 2001, pp. 35-53.

[10] Gong G, Entekhabi D, Cohen J (2003) Relative impacts of Siberian and North American snow anomalies on the winter Arctic Oscillation. Geophysical Research Letters 30(16):1848–1851

[11] Groisman, P. Ya. and T. D. Davies. "Snow cover and the climate system," in: H. G. Jones, J. W. Pomeroy, D. A. Walker, and R. W. Hoham, eds., The Ecology of Snow.Cambridge, UK: Cambridge University Press, 2000, pp. 1-44.

[12] Hall, D. K., Riggs, G. A., Salomonson, V. V.," Development of methods for mapping global snow cover using moderate resolution imaging spectroradiometer data", Remote Sens. Environ., 54(2), 127–140(1955)[doi:10.1016/0034-4257(95)00137-P, 1995.]

[13] Hall, Dorothy K., George A. Riggs, and Vincent V. Salomonson. 2007, updated daily. MODIS/Aqua Snow Cover 8-Day L3 Global 0.05deg CMG V005, [list the dates of the data used]. Boulder, Colorado USA: National Snow and Ice Data Center. Digital media.

[14] IPCC (2001) Climate Change 2001: The scientific basis. Contribution of working group I to the third assessment report ofthe Intergovernmental Panel on Climate Change. WMO/ UNEP. Cambridge University Press, Cambridge, 944 pp

[15] Judah cohen, David Rind ,the effect of snow cover on the climate, Journal of climate, July, 1991, PP:689-706

[16] Kripalani, R.H. and A. Kulkarni 1999: Climatology and variability of historical Soviet snow depth data: some new perspectives in snow-Indian monsoon tele-connections. Clim. Dyn., 15, 475-489.

[17] Matthew H. Savoie, Richard L. Armstronga, Mary J. Brodzika and James R. Wang, Atmospheric corrections for improved satellite passive microwave snow cover retrievals over the Tibet Plateau, Remote Sensing of Environment,vol.113, no. 15, PP.2661-2669,2009

[18] Menon, S., Koch, D., Beig, G., Sahu, S., Fasullo, J., Orlikowski, D.,"Black carbon aerosols and the third polar ice cap", Atmos. Chem. Phys., 10, 4559–4571(2010) [doi:10.5194/acp-10-4559-2010, 2010.]

[19] National Ice Center. 2008, updated daily. IMS daily Northern Hemisphere snow and ice analysis at 4 km and 24 km resolution. Boulder, CO: National Snow and Ice Data Center. Digital media.

[20] Nolin, A., R. L. Armstrong, and J. Maslanik. 1998, updated daily. Near-Real-Time SSM/I-SSMIS EASE-Grid Daily Global Ice Concentration and Snow Extent, [list the dates of the data used]. Boulder, Colorado USA: National Snow and Ice Data Center. Digital media.

[21] Pulliainen, J., Grandell, J., Hallikainen, M., "HUT snow emission model and its applicability to snow water equivalent retrieval". IEEE Transactions on Geoscience and Remote Sensing, vol. 37, no. 3, pp. 1378-1390, 1999.

[22] Qin Dahe, Liu Shiyin, Li Peiji, 2006: Snow Cover Distribution, Variability, and Response to Climate Change in Western China. J. Climate, 19, 1820–1833

[23] Qiu Yubao, Jiancheng Shi, Juha Lemmetyinen, Anna Kontu, Jouni Pulliainen, Huadong Guo,Lingmei Jiang, James R. Wang, Martti Hallikainen, Li Zhang，the atmosphere influence to AMSR-E measurements over snow-covered areas: simulation and experiments, Proceedings of IGARSS'09, 13-17 July, Cape Town, Africa, 2009

[24] Riggs GA, Hall DK, Salomonson VV (2003) MODIS snow products user guide for collection 4 data products. Available at http://modis-snow-ice.gsfc.nasa.gov

[25] Roger G.Barry, The Role of Snow and Ice in the Global Climate System: A Review, Polar Geography, Volume 26, Number 3, 1 July 2002 , pp. 235-246(12)

[26] Serreze M, Walsh J, Chapin III F, Osterkamp T, Dyurgerov M, Romanosky V, Oechel W, Morison J, Zhang T, Barry R (2000) Observational evidence of recent change in the northern high-latitude environment. Climatic Change 46:159–207.

[27] Steve Vavrus, The role of terrestrial snow cover in the climate system, Clim Dyn (2007) 29:73–88, DOI 10.1007/s00382-007-0226-0

[28] Tedesco, Marco, Richard E. J. Kelly, James L. Foster, and Alfred T. C. Chang. 2004, updated daily. AMSR-E/Aqua Daily L3 Global Snow Water Equivalent EASE-Grids V002, 2002~2010. Boulder, Colorado USA: National Snow and Ice Data Center. Digital media.

[29] Walsh, J. E. "Large-scale effects of seasonal snow cover," in B. E. Goodison, R. G. Barry, and J. Dozier, eds., Large Scale Effects of Seasonal Snow Cover. Wallingford, UK: IAHS Press, IAHS Publ. No. 166, 1987, pp. 3-14. Wang, X., Xie, H., Liang, T., "Evaluation of MODIS snow cover and cloud mask and its application in Northern Xinjiang, China", Remote Sens. Environ., 112, 1497–1513(2008) [doi:10.1016/j.rse.2007.05.016, 2008.]

[30] Wulder M A, Nelson T A, Derksen C, Seemann D, Snow cover variability across central Canada (1978-2002) derived from satellite passive microwave data, Climatic Change (2007), Volume: 82, Issue: 1-2, Publisher: Springer, Pages: 113-130

[31] Xu Changchun; Yaning, Chen; Weihong, Li; Yapeng, Chen; Hongtao, Ge, Potential impact of climate change on snow cover area in the Tarim River basin, Environmental Geology, 2007,Volume 53, Issue 7, pp.1465-1474

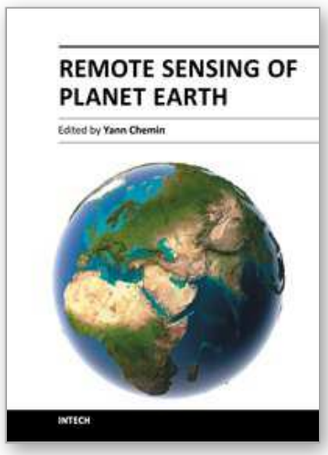

Remote Sensing of Planet Earth

Edited by Dr Yann Chemin

ISBN 978-953-307-919-6
Hard cover, 240 pages
Publisher InTech
Published online 27, January, 2012
Published in print edition January, 2012

Monitoring of water and land objects enters a revolutionary age with the rise of ubiquitous remote sensing and public access. Earth monitoring satellites permit detailed, descriptive, quantitative, holistic, standardized, global evaluation of the state of the Earth skin in a manner that our actual Earthen civilization has never been able to before. The water monitoring topics covered in this book include the remote sensing of open water bodies, wetlands and small lakes, snow depth and underwater seagrass, along with a variety of remote sensing techniques, platforms, and sensors. The Earth monitoring topics include geomorphology, land cover in arid climate, and disaster assessment after a tsunami. Finally, advanced topics of remote sensing covers atmosphere analysis with GNSS signals, earthquake visual monitoring, and fundamental analyses of laser reflectometry in the atmosphere medium.

InTech Europe
University Campus STeP Ri
Slavka Krautzeka 83/A
51000 Rijeka, Croatia
Phone: +385 (51) 770 447
Fax: +385 (51) 686 166
www.intechopen.com

InTech China
Unit 405, Office Block, Hotel Equatorial Shanghai
No.65, Yan An Road (West), Shanghai, 200040, China
中国上海市延安西路65号上海国际贵都大饭店办公楼405单元
Phone: +86-21-62489820
Fax: +86-21-62489821

IntechOpen